

## Robust classification using balanced networks

**Julian Büchel**

JUBUECHE@ETHZ.CH

*SynSense*

*Thurgauerstrasse 40*

*Zürich, ZH, Switzerland*



## Contents

|          |   |           |
|----------|---|-----------|
| <b>1</b> | <b>Learning in adaptive non-linear control theory</b> | <b>5</b>  |
| <b>2</b> | <b>Learning arbitrary dynamical systems in EBN's</b>  | <b>5</b>  |
| <b>3</b> | <b>Training a classifier based on an EBN</b>          | <b>6</b>  |
| <b>4</b> | <b>Results</b>  | <b>9</b>  |
| 4.1      | Temporal XOR . . . . .                                | 9         |
| 4.2      | Wake-phrase detection . . . . .                       | 10        |
| 4.3      | Robustness . . . . .                                  | 13        |
| 4.4      | Role of $\Omega^f$ . . . . .                          | 15        |
| <b>5</b> | <b>Discussion</b>                                     | <b>17</b> |

## Abstract

In balanced networks, excitatory and inhibitory currents are matched on either a long or short timescale and lead to sparse and irregular firing patterns, often observed in cortical neurons. In Bourdoukan et al. (2012), a pre-defined network architecture is derived from the condition that a neuron only spikes if it contributes to reducing the representation error of some input signal. This precise network architecture leads to a robust, energy efficient and precise signal representation that can be augmented with additional recurrent weights to perform more complex tasks.

While it has been shown that these networks can be used to implement linear (Boerlin et al. (2013)) or even non-linear dynamical systems (Alemi et al. (2017)), no paper has shown a way to train a classifier using efficient balanced networks (EBN) as a foundation. In this paper, we demonstrate how a tightly balanced network can learn to do arbitrary classification tasks of varying complexity, while still keeping the benefits of the balanced network presented in Bourdoukan et al. (2012).

## 1. Learning in adaptive non-linear control theory

Let us assume an arbitrary dynamical system of the form

$$\dot{x} = f(x) + c(t) \quad (1)$$

where  $x$  is a vector of state variables  $x_j$ ,  $f(\cdot)$  is a non-linear function (e.g.  $\tanh(\cdot)$ ), and  $c$  is a time-dependent input of the same dimensionality of  $x$ . Furthermore, let us assume a "student" dynamical system of the form

$$\dot{\hat{x}} = -\lambda\hat{x} + \mathbf{W}^T\Psi(\hat{x}) + c(t) + ke \quad (2)$$

where  $\hat{x}$  is a vector of state variables  $\hat{x}_j$ ,  $\lambda$  is a leak term, and  $c$  is the same time-dependent input as in Equation 1. Over time, the signed error  $e = x - \hat{x}$  between the teacher dynamics (Eq. 1) and the student dynamics (Eq. 2) is computed and fed into the student dynamics, causing the student state variables  $\hat{x}$  to follow the target variables  $x$  more closely. This close tracking enables us to update the weights  $\mathbf{W}$  using Eq. 3, so that over the course of learning, the factor  $k$  can be reduced to zero and the network follows the teacher dynamics autonomously, using only a weighted sum of basis functions, given by  $\Psi(\hat{x}) = \phi(\mathbf{M}\hat{x} + \theta)$ , for some non-linear function  $\phi$ , and some random  $\mathbf{M}$  and  $\theta$ . The learning rule used to adapt the weights  $\mathbf{W}$  is given by

$$\dot{\mathbf{W}} = \eta\Psi(\hat{x})e^T \quad (3)$$

and can be shown to let the weights  $\mathbf{W}$  converge towards the optimal weights, denoted  $\mathbf{W}^{\text{true}}$ , assuming that the input  $c(t)$  does not lie on a low-dimensional manifold and that the student system has enough high-dimensional basis functions. For more information and a proof of the above statement, see Alemi et al. (2017). It should be noted that the relation between  $x$  and  $c$  should be well-defined by an autonomous (non-)linear dynamical system of the form  $\dot{x} = f(x) + c(t)$  and that one cannot simply assume a "black box" dynamical system implementing *any* relation of the form  $\dot{x} = \mathcal{B}(x, c)$ . Concretely, in the light of classification, one cannot simply assume there exists an autonomous dynamical system relating the input  $c$  to some target response variable, and that this relation can be learned by the learning rule described above. This observation is important, as it makes it harder to build a classifier given the tools described above. In the next section, we will review how a network of spiking neurons can implement the above learning rule in order to learn the dynamics of a teacher dynamical system.

## 2. Learning arbitrary dynamical systems in EBN's

In this section, we will briefly recapitulate how an efficient balanced network of spiking neurons can learn to implement any non-linear dynamical system of the form  $\dot{x} = f(x) + c(t)$ . We will assume that, given a network of  $N$  neurons, one can use a decoder  $\mathbf{D}$  to reconstruct the target variable from the filtered spike trains of the population using  $\hat{x} = \mathbf{Dr}$ , so that  $x \approx \hat{x}$ .

Derived from the fact that in an efficient balanced network (Bourdoukan et al. (2012)), a neuron only fires a spike if it contributes to reducing the loss  $L$ , given by

$$L = \frac{1}{T} \sum_{t=0}^T \|x(t) - \hat{x}(t)\|_2^2 + \mu\|r(t)\|_2^2 + \nu\|r(t)\|_1$$

the membrane potentials in the network are defined by

$$V(t) = \mathbf{D}^T x(t) - D^T Dr(t) - \mu r(t) \quad (4)$$

Following Alemi et al. (2017), we differentiate Eq. 4 and substitute  $\dot{r}(t) = -\lambda r(t) + o(t)$ ,  $\dot{x}(t) = f(x(t)) + c(t)$  and  $\hat{x} = \mathbf{D}r$  to get

$$\begin{aligned} \dot{V}(t) &= -\lambda V(t) + \mathbf{D}^T(f(x(t) + c(t))) - \mathbf{D}^T\mathbf{D}(-\lambda r(t) + o(t)) - \mu(-\lambda r(t) + o(t)) \\ &= -\lambda V(t) + \mathbf{D}^T c(t) - (\mathbf{D}^T\mathbf{D} + \mu I)o(t) + \mathbf{D}^T(\lambda \hat{x} + f(x)) \end{aligned}$$

We then approximate the term  $\lambda \hat{x} + f(x)$  [Not sure here. In the paper it is  $\lambda x + f(x)$ , but I can't derive it] by a weighted set of basis functions, given by  $\Omega^s \Psi(r)$ , where  $\Psi(r) = \phi(\mathbf{M}r + \theta)$ . We note that in our simulations, we omitted the term  $\Psi(r)$  and simply replaced it with the population spike trains  $o(t)$ .

By feeding the error term  $e = x - \hat{x}$  back into the network using the feed-forward weights  $\mathbf{D}^T$ , we obtain the final network dynamics

$$\dot{V}(t) = -\lambda V(t) + \mathbf{F}c(t) - \Omega^f o(t) + \Omega^s o(t) + k\mathbf{D}^T e(t)$$

where the feed-forward weights  $\mathbf{F}$  are given by  $\mathbf{D}^T$  and the optimal fast recurrent weights by  $\Omega^f = -(\mathbf{D}^T\mathbf{D} + \mu I)$ .

Similar to the case in control-theory, the learning rule for the slow recurrent weights is given by

$$\dot{\Omega}^s = \eta \Psi(r)(\mathbf{D}^T e)^T$$

where we simply replaced  $\Psi(r)$  with  $r$ .

To speed up the simulations, we assumed that the accumulated updates to  $\Omega^s$ , given by  $\sum_{t=0}^T \eta \Psi(r)(\mathbf{D}^T e)^T$  are approximately the same as accumulating the rates and errors into large arrays of size  $N \times T$  and performing the update in a batched fashion, after a whole signal was evaluated rather than after every timestep:

$$\dot{\Omega}^s = \eta \mathbf{R}(\mathbf{D}^T \mathbf{E})^T$$

### 3. Training a classifier based on an EBN

The coding properties of efficient balanced networks make them attractive for many applications, especially in the neuromorphic community. However, so far it has only been shown how to implement linear and non-linear dynamical systems of a specific form using EBNs. In this section we provide a method to train an efficient balanced network to perform classification tasks of varying complexity.

Let us define our time-varying, real-valued input as  $c_t$ , where  $c \in \mathcal{R}^{N_c \times 1}$  and  $t \in \{0..T\}$ . The goal of training a classifier is to find a mapping  $f(\Theta)$  that maps any input  $\mathbf{c}$  to the

desired target variable  $\mathbf{y}$ , where  $\mathbf{y}$  is an indicator variable over time. For simplicity, we will consider the case of binary classification. We however note that our method can be easily extended to a multi-class classification task.

Considering the ability of the learning rule presented in section 2, one might be inclined to assume a "black box" dynamical system  $\mathcal{B}$  of the form  $\dot{y} = f(y) + c(t)$  that, given input  $\mathbf{c}$ , autonomously produces the desired target  $\mathbf{y}$ . Two problems come with this approach: 1) The dynamical system is not well-defined, as it is no-longer explicitly defined by a teacher dynamical system. Furthermore, the system is autonomous, as the function  $f(\cdot)$  does not depend on the input, but only on past values of the target variable, making it impossible for the system to find a complex relationship between input and target. 2) This approach assumes that the input and target variable have the same number of dimensions, which is almost never the case.

How can we use the above learning rule to train an efficient balanced network to perform arbitrary classification tasks at low metabolic cost, high robustness and good classification performance?

To answer this question, we consider a simple rate network consisting of  $\hat{N}$  units, following

$$\tau_j \dot{x}_j = -x_j + \hat{\mathbf{F}}c(t)_j + \hat{\Omega}f(x(t))_j + b_j + \epsilon_j \quad (5)$$

where  $\tau_j$  is the time constant of the  $j$ -th unit,  $\hat{\mathbf{F}}$  are feed-forward weights of shape  $\hat{N} \times N_c$ ,  $c(t)$  is the  $N_c$  dimensional input at time  $t$ ,  $f(\cdot)$  is a non-linear function (e.g.  $\tanh(\cdot)$ ),  $\hat{\Omega}$  are recurrent weights of shape  $\hat{N} \times \hat{N}$  and  $b_j$  and  $\epsilon_j$  are bias and noise terms, respectively. We observe that a rate network can be written in the general form  $\dot{x} = \tilde{f}(x) + \tilde{c}(t)$ , with  $\tilde{f}(x) = 1/\tau(-x + \hat{\Omega}fx(t)) + \epsilon$  and  $\tilde{c}(t) = 1/\tau(\hat{\mathbf{F}}c(t) + b)$ , meaning that an efficient balanced network can be trained to implement the dynamics of *any* given rate network obeying the dynamics of Eq. 5.

Let us now restate the dynamics of the spiking network with adapted notation for ease of understanding:

$$\dot{V}(t) = -\lambda V(t) + \mathbf{F}\tilde{c}(t) - \boldsymbol{\Omega}^f o(t) + \boldsymbol{\Omega}^s o(t) + k\mathbf{D}^T e(t)$$

And let us assume that we have trained a rate nework receiving inputs  $\mathbf{c}$  to successfully produce a good approximation  $\hat{\mathbf{y}} = \hat{\mathbf{D}}\mathbf{x}$  of the target variable  $\mathbf{y}$ , so that  $\hat{\mathbf{y}} \approx \mathbf{y}$ .

We now see that we can train a network of spiking neurons to encode the *dynamics*  $\mathbf{x}$  of the rate network, by giving the spiking network input  $\tilde{c}(t) = 1/\tau(\hat{\mathbf{F}}c(t) + b)$ . This makes the *dynamics* of the rate network the new target of the spiking network:  $\tilde{\mathbf{x}} = \mathbf{D}r$ , so that  $\tilde{\mathbf{x}} \approx \mathbf{x}$ . After the recurrent weights  $\boldsymbol{\Omega}^s$  have been learned to implement a network that encodes the rate-network dynamics, classification can be performed by the simple computation  $y(t) = \hat{\mathbf{D}}\mathbf{D}r(t)$ , where  $\hat{\mathbf{D}}$  are the rate-network read-out weights,  $\mathbf{D}$  are the spiking read-out weights and  $r(t)$  are the filtered spike trains at time  $t$  of the spiking network.

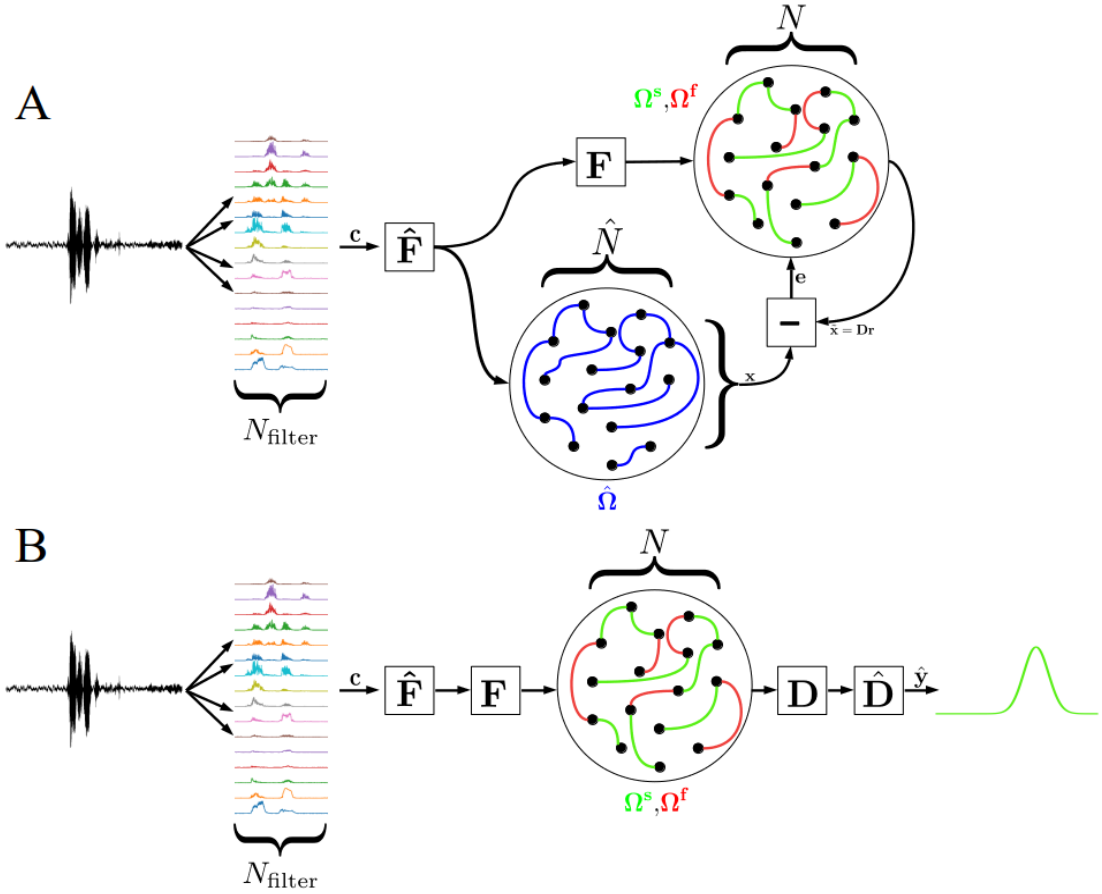


Figure 1: A high-level illustration of the training (**A**) and inference (**B**) process using the presented framework for an auditory classification task. **A:** During training, auditory samples are filtered using a set of band-pass filters with varying cut-off frequencies to produce a 16 channel input, denoted  $\mathbf{c}$ . This input is then fed into the pre-trained rate network, which does inference on the presented signal. The dynamics  $\mathbf{x}$  produced by the rate network are then used to compute the error  $\mathbf{e} = \mathbf{x} - \hat{\mathbf{x}}$ , which is then fed back into the spiking network using the feed-forward weights  $\mathbf{D}^T$ . Simultaneously, the spiking network receives the same input as the rate network, simply projected by the feed-forward weights  $\mathbf{F} = \mathbf{D}^T$ . Using the read-out weights  $\mathbf{D}$ , it then produces an estimation of the rate network dynamics  $\hat{\mathbf{x}}$ , which is then used to compute the error.

The inference mode, depicted in **B**, is straightforward: The now trained spiking network receives the same input the rate network would receive, but transformed using the feed-forward weights  $\mathbf{F}$ . It then produces the network dynamics  $\tilde{\mathbf{x}} = \mathbf{D}\mathbf{r}$  that closely match the ones of the rate network (if it would have received the signal) and produces the output  $\tilde{\mathbf{y}} = \hat{\mathbf{D}}\tilde{\mathbf{x}}$ . The value  $\tilde{\mathbf{y}}$  is then thresholded to obtain the final prediction.

## 4. Results

### 4.1 Temporal XOR

In this experiment, a rate network of 64 neurons was trained to perform temporal XOR on a one-dimensional input. The network was presented with two bumps of magnitude  $\pm 1$ , indicating True or False. The bumps had a variable length between 100 and 230ms. The target response was chosen to be a smoothed step function.

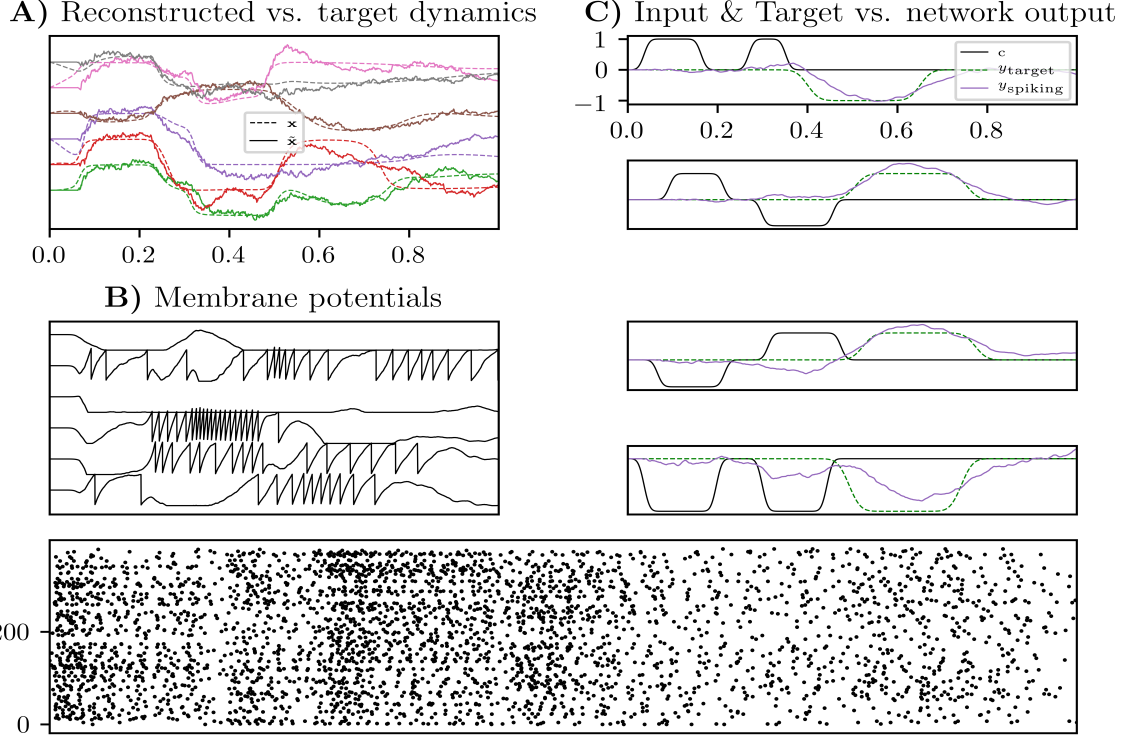


Figure 2: **A:** The spiking network consisting of 380 neurons (6 times  $\hat{N}$ ) successfully reconstructs the dynamics of the rate network. **B:** The membrane potentials and spike trains show irregular and distributed spiking activity, although no fast recurrent connections were used. **C:** The final output of the network is computed using the read-out matrix from the rate network and the reconstructed dynamics of the spiking network. Our network successfully learns the non-linear dynamics of the rate network to a precision high enough to predict the temporal XOR target with negligible error.

In practice, we found that using a narrow target response degrades performance drastically since the dynamics of the rate network are more abrupt. Usually, having longer target responses yields smoother rate network dynamics, which makes it easier for the spiking network to learn. Our network learns this temporal XOR task to 99.99% accuracy using only 6 times as many neurons as the rate network. We however note that the input space is very small and that both networks might simply overfit to the generated data. One

aspect that we would like to highlight at this point is the fact that we are not using any dendritic non-linearity, meaning that we simply replaced the term  $\Psi(r)$  with  $r$ . Because of the non-linearity of the neuron dynamics, using the spiking rates as a basis function suffices to learn the dynamics of a rate network using  $\tanh(\cdot)$  as a non-linear activation function. We also note that the EBN connections,  $\Omega^f$ , do not improve reconstruction accuracy, but do improve robustness against sudden neuron death (see Alemi et al. (2017)) as we show in a later section.

#### 4.2 Wake-phrase detection

To show that our approach also works on a more complex and realistic task, we used a network consisting of  $N = 768$  spiking neurons that learned to imitate a rate network with  $\hat{N} = 128$  units. Contrary to approaches like reservoir computing, our network operates in a precise spike-timing fashion, allowing us to use only 5-10 times as many spiking neurons as the rate network. The rate network was trained to recognize a wake-phrase using roughly 10k training samples and 5k validation and testing samples. While the rate network achieved a testing accuracy of 90%, our spiking imitator achieved 87% after training for only 10 epochs on about 1000 training samples. We found that for training our network a learning rate schedule of the form  $f(t) = ae^{(-t/b)} + c$  worked best, where  $a = \eta_{\text{initial}}$ ,  $c = \eta_{\text{end}}$  and  $b = (T/2)/\ln(100)$  with  $T$  being the total number of signal iterations. For the experiments conducted in this section, we chose  $\eta_{\text{initial}} = 1e - 4$  and  $\eta_{\text{end}} = 1e - 6$ . We also realized that having a schedule for the factor  $k$  that controls the amount of error-feedback current is of high importance: A constantly high  $k$  results in no generalization during training since the network dynamics are governed by the error-feedback current and a too low  $k$  does not give the slow recurrent weights a chance to update correctly since the network is far from following the desired dynamics. For these reasons, having a schedule for  $k$  is extremely important. For this experiment, we chose a step function that decrements  $k$  by a fixed amount after some number of signal iterations. The reason we chose a step function is the following: If  $k$  is constantly changing, even slowly, the amount of error-feedback current that "helps" the network is constantly changing as well and does not give the slow recurrent weights a chance to adapt to the amount of "helper-current" that is present in the network. We achieved best performance when we gave the slow recurrent weights some time to adapt to the current level by just keeping  $k$  constant for some time before decreasing it again.

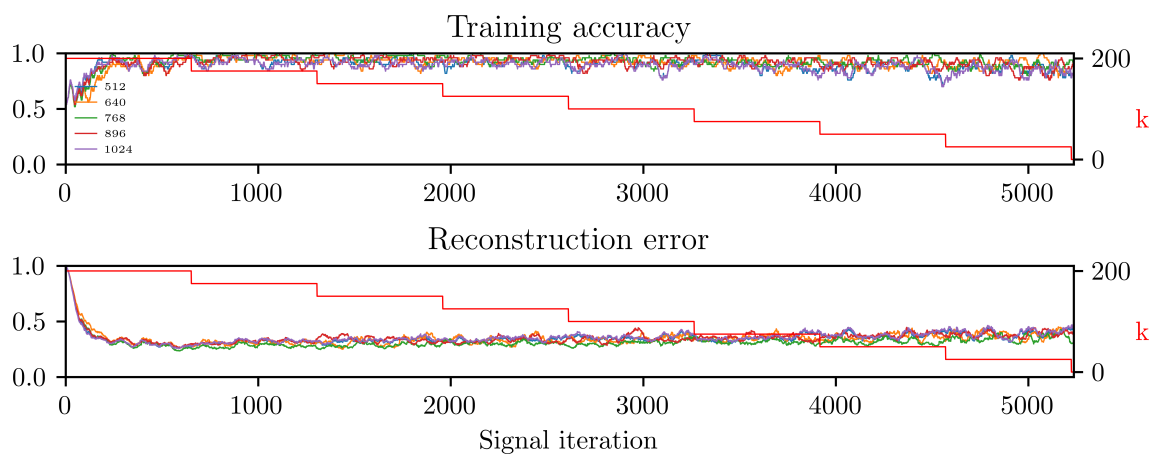


Figure 3: As  $k$  is slowly decreasing, the helping error current  $I_{kDTe}$  becomes negligible and the network must generalize. During this process, the reconstruction error and the training accuracy increases/decreases a little bit.

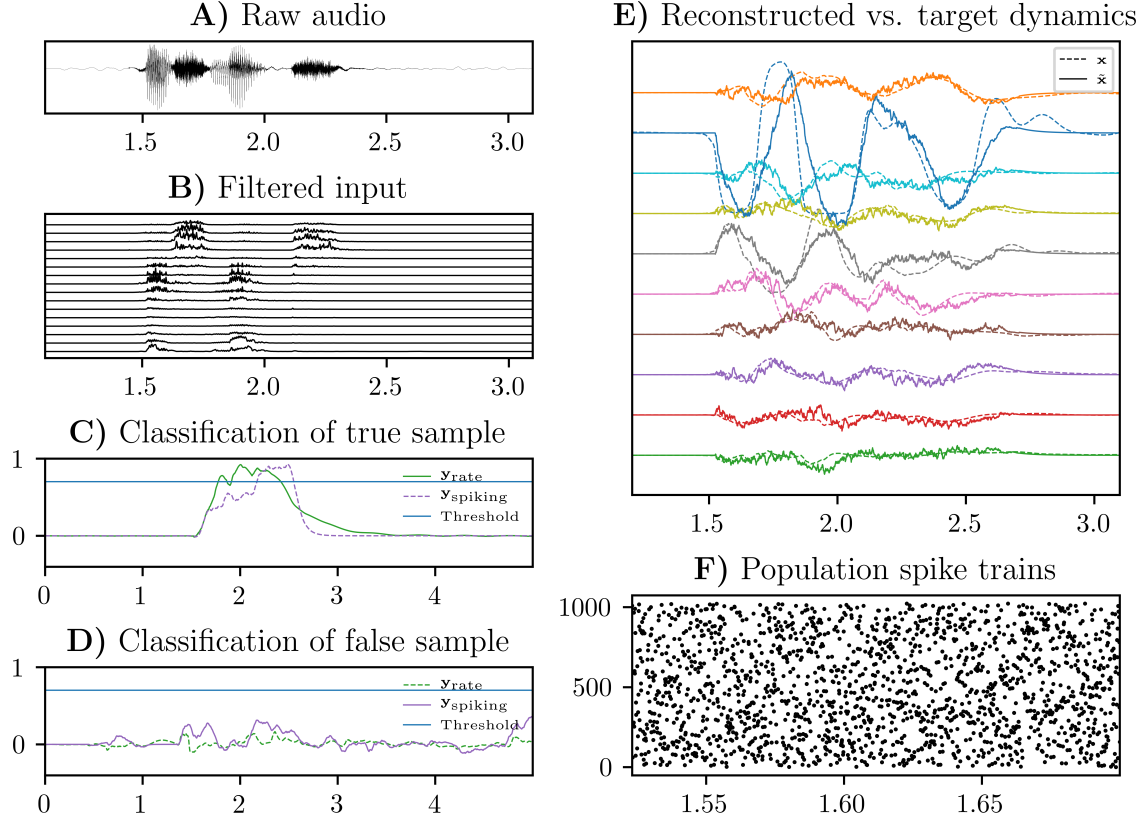


Figure 4: **A:** Audio samples either containing a key phrase, like "Wake up!", or plain talking were presented to the network, which then had to decide whether the input was the target phrase or not. **B:** To make classification easier, 16 butterworth filters with different cutoff frequencies were applied to create a 16-dimensional input signal. **C:** For a sample containing the key phrase, our network output closely follows the output of the rate network and thus makes the correct decision. In this experiment, a threshold at 0.7 determined whether the prediction was positive or negative. **D:** Negative samples on the other hand did not cause a rise in the output variable and were therefore correctly classified as negative samples. For this particular experiment, the rate network achieved 90.31% on a held out test set containing 1000 samples. The spiking network achieved 86.80% test accuracy, while imitating the dynamics of the rate network (**E**). **F:** As expected, the spiking activity of the network is distributed and does not exhibit any output dependent patterns. For this experiment, 1024 neurons were used.

### 4.3 Robustness

On analog mixed-signal neuromorphic hardware components are not identical, which leads to a distribution of parameters such as time constants or spiking thresholds. In this experiment, we simulated component mismatch by distributing the synaptic- and membrane time-constants, as well as the spiking thresholds using a Gaussian distribution with mean equal to the original value and the standard deviation being 20% of the mean. Figure 7 demonstrates this behavior by plotting the distributions of membrane time-constants on multiple cores on a neuromorphic processor, obtained through oscilloscope recordings. Figure 6 shows the robustness of the network to component mismatch and sudden neuron failure for 300ms. Since neuromorphic processors, analog or digital, are furthermore constrained in the resolution of their weights, which also can be seen as a type of noise, we reduced the total weights to 2, 3 and 4 bit floating point values. To integrate the low-resolution weights into training, we kept a full-precision version of the weights and adapted them using the updates computed from the low-resolution network. Not surprisingly, this method yields much better results than just reducing the precision of the weights post-learning. Table 4.3 shows the testing accuracies for 1000 samples using the networks perturbed by various noise sources and Figure 5 shows a box plot of the same results.

| Original          | Quantised to 4 bits | Quantised to 3 bits | Quantised to 2 bits | Rate network       |
|-------------------|---------------------|---------------------|---------------------|--------------------|
| $86.80 \pm 0.7\%$ | $86.37 \pm 0.68\%$  | $86.31 \pm 0.88\%$  | $82.87 \pm 1.04\%$  | $90.31 \pm 0.48\%$ |

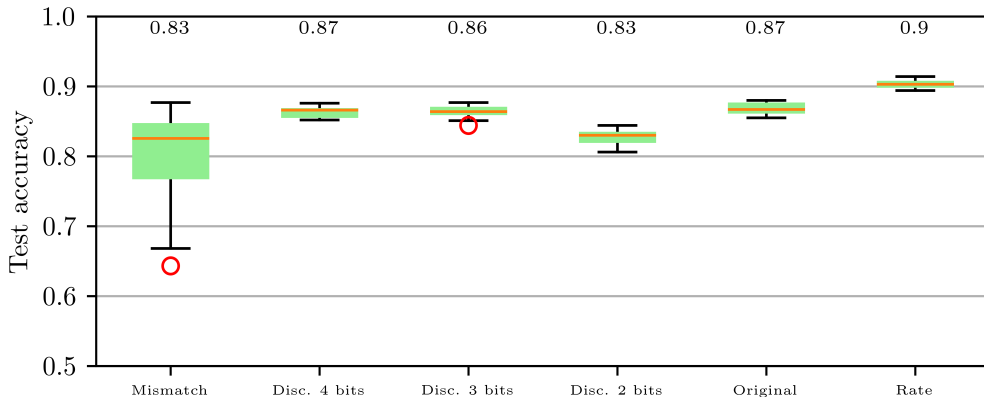


Figure 5: Test accuracies over 13 trials on 1000 samples for a network of 768 neurons perturbed by different kinds of noise.

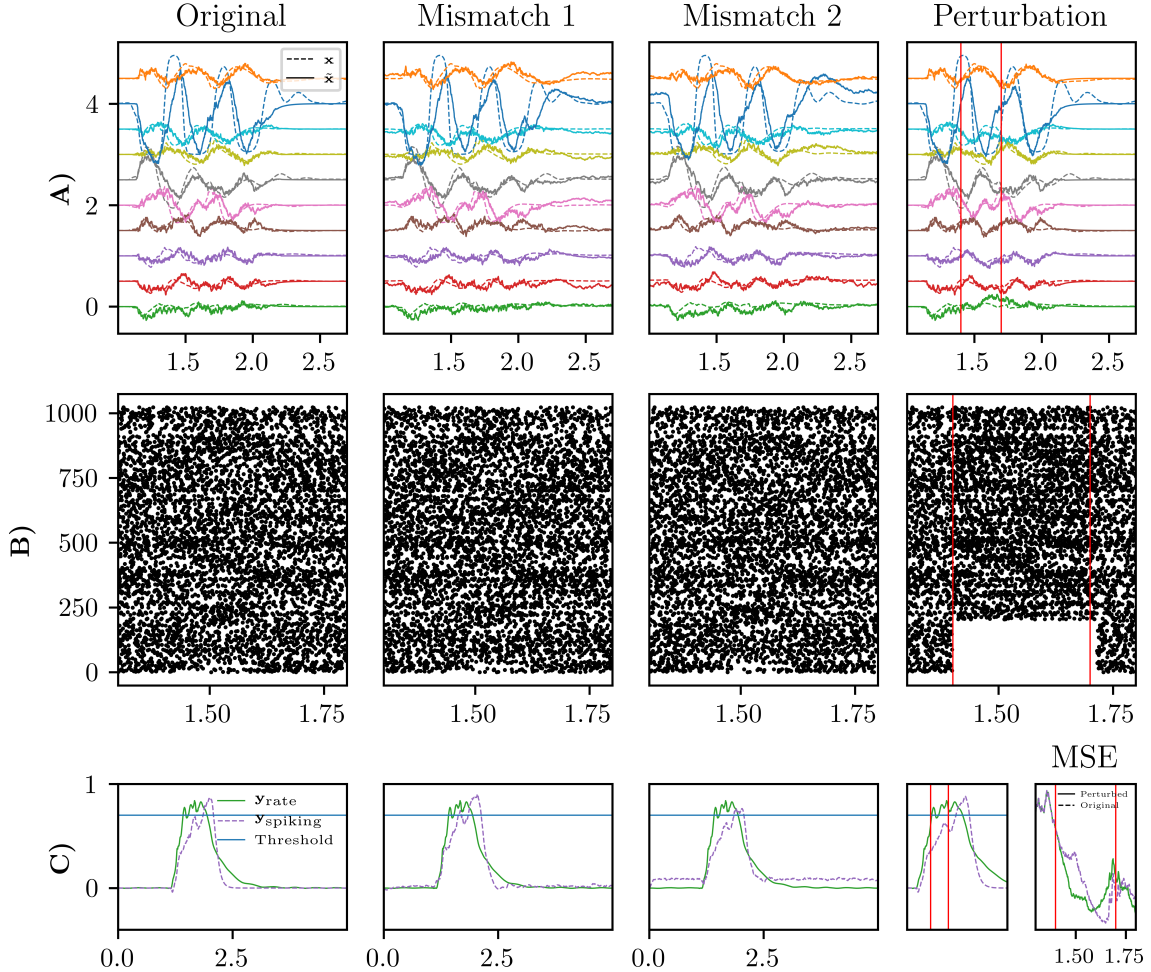


Figure 6: **A:** Reconstruction of the 128-dimensional target dynamics (only first 10 dimensions are shown). **B:** Here, one can observe the effect of the mismatch on the recurrent dynamics. Due to the distribution of the neuron- and synaptic time-constants, recurrent activity is sustained a little longer with some individual neurons spiking at a higher frequency. In the last network instance, we clamped 20% of the neurons at a crucial time during classification. However, as can be seen in **C**, the reconstruction is stable, as well as the final output. It should also be noted that for 20% clamped neurons, the mean-squared error (MSE) did not increase during the time the neurons were shut off.

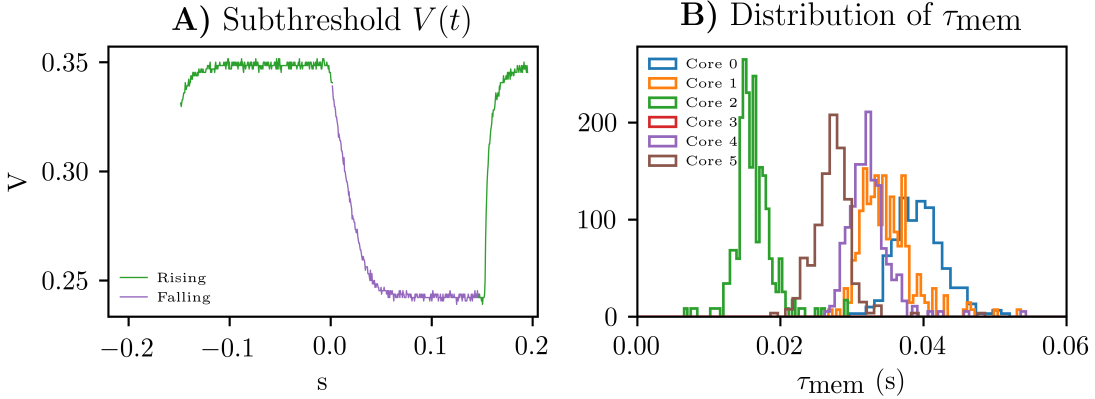


Figure 7: **A:** Recording of a neurons membrane potential on an analog mixed-signal neuromorphic chip. **B:** The membrane time-constants of neurons for different expected time-constants. It can be seen that as the time constant increases, also the standard deviation increases (thus  $\sigma = 0.2\mu$ ). The time-constants were computed by fitting an exponential to subthreshold recordings of each neuron.

Figure 8 shows the performance of two networks using  $N = 1024$  and  $N = 768$  neurons after simulated mismatch was applied to the involved time constants and spiking thresholds. We found that robustness to mismatch increases with the number of neurons used.

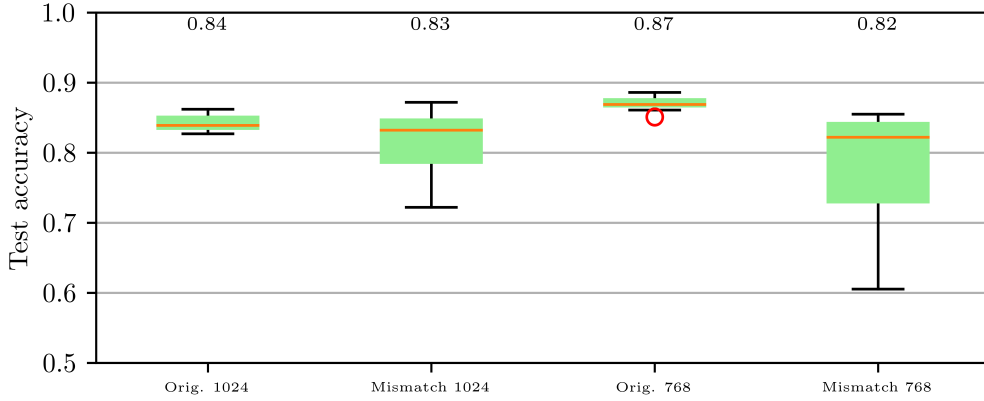


Figure 8: Mismatch robustness of a network with 1024 (l) and 768 (r) neurons.

#### 4.4 Role of $\Omega^f$

As previously stated in section 2, we found that our network is able to reconstruct the non-linear dynamics of a rate network *without* the dendritic non-linearities  $\phi(\mathbf{M}r + \theta)$  and *without* the fast connections  $\Omega^f$ . If anything, we found that using the EBN connections

leads to a degradation in accuracy as Figure 9 illustrates. From Bourdoukan et al. (2012), we know that EBNs lead to sparser and more distributed spike trains and result in a lower reconstruction error in an autoencoder-like setting. We therefore, prior to training, compared the spike-trains, membrane potentials and reconstruction error of a network with and without  $\Omega^f$  to make sure that our EBN actually met these expectations. Although the reconstruction error of the EBN was lower than the standard network (with  $\Omega^s$  set to  $\mathbf{0}$ ), the network without  $\Omega^f$  constantly showed a lower reconstruction error.

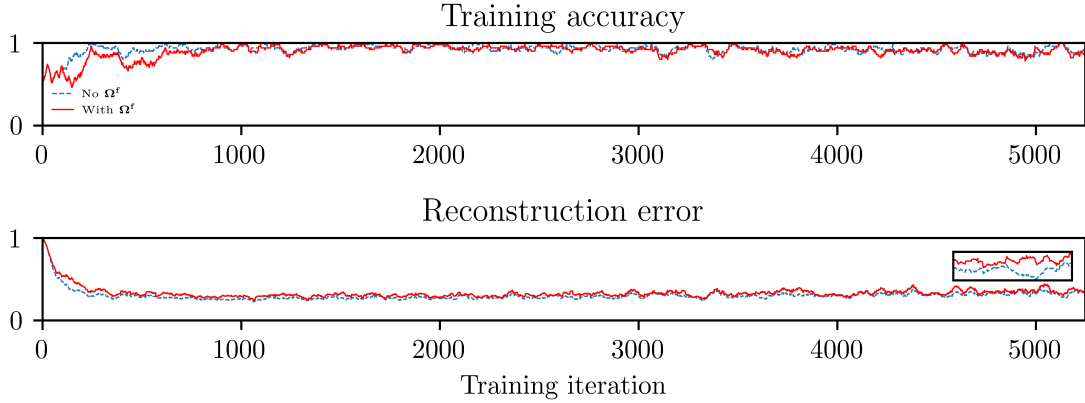


Figure 9: Training accuracy (top) and reconstruction error (bottom) over the course of training for a network with and without  $\Omega^f$ .

Similar to the findings in Alemi et al. (2017), we could however show that a network with  $\Omega^f$  had a much lower reconstruction error when a certain percentage of neurons is clamped to  $V_{\text{rest}}$  as Figure 10 shows.

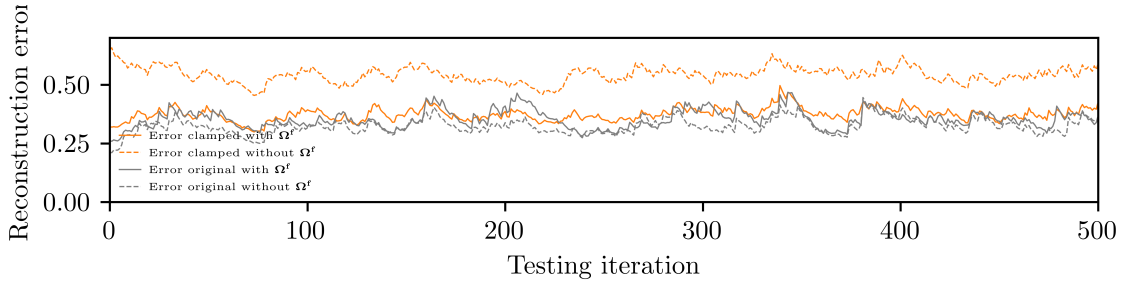


Figure 10: The reconstruction error of the "clamped" network with  $\Omega^f$  is constantly lower than the one without  $\Omega^f$ , while the reconstruction error for the original network without  $\Omega^f$  has lower reconstruction error and therefore better classification accuracy.

## 5. Discussion

## References

- Alireza Alemi, Christian Machens, Sophie Denève, and Jean-Jacques Slotine. Learning arbitrary dynamics in efficient, balanced spiking networks using local plasticity rules, 2017.
- M. Boerlin, C. K. Machens, and S. Denève. Predictive coding of dynamical variables in balanced spiking networks. *PLoS Comput. Biol.*, 9(11):e1003258, 2013.
- Ralph Bourdoukan, David G. T. Barrett, Christian K. Machens, and Sophie Denève. Learning optimal spike-based representations. In *Proceedings of the 25th International Conference on Neural Information Processing Systems - Volume 2*, NIPS'12, pages 2285–2293, USA, 2012. Curran Associates Inc. URL <http://dl.acm.org/citation.cfm?id=2999325.2999390>.